Inorg. Chem. **2004**, *43*, 2597–2610

DFT and Metal–Metal Bonding: A Dys-Functional Treatment for Multiply Charged Complexes?

Simon Petrie and Robert Stranger*

Department of Chemistry, The Faculties, The Australian National University, Canberra ACT 0200, Australia

Received May 16, 2003

Density functional theory (DFT) calculations are reported for 16 binuclear transition-metal complexes. Structural motifs studied include face-shared and edge-shared bioctahedra, carboxylate-bridged "paddlewheel" complexes, and nonbridged dimers possessing direct metal–metal bonds. Most of these structure types are represented both by multiply charged (tri- and tetra-anionic, and tetracationic) and by neutral or singly charged examples. Geometry optimizations for these species, in the vacuum phase, use the "broken-symmetry" approach coupled with nine different DFT methods. We find a clear dichotomy in the performance of different DFT approaches. For the eight neutral or singly charged complexes, orthodox gradient-corrected DFT methods such as BP and PBE perform generally very well in reproducing in vacuo the complex geometries obtained from X-ray crystallographic studies. In contrast, these orthodox approaches fail to reliably mimic the crystalline geometries for more highly charged complexes such as $Mo_2Cl_9^{3-}$, $Cr_2(CH_3)_8^{4-}$, and $Rh_2(NCCH_3)_{10}^{4+}$. Much closer agreement with experimental condensed-phase structures for the multiply charged dinuclear complexes is seen for two "local-density-approximation" approaches, Xα and VWN, and for VWN+B-LYP, an unorthodox combination of the VWN local and B-LYP nonlocal density functionals. The very good performance of the latter approaches arises from an essentially fortuitous cancellation of errors: while the generally overbinding nature of these approaches suggests that they will not reliably describe true gas-phase structures, this overbinding compensates very well for the coulombic distortion expected when complexes are removed from the charge-stabilizing environment of the crystalline or solvated state. We recommend that, as an alternative to the (computationally expensive) incorporation of solvent-field corrections, VWN+B-LYP is the preferred method for structural characterization of triply or more highly charged dinuclear complexes, while orthodox approaches such as PBE perform best for neutral or mildly charged complexes.

Introduction

Incomplete occupation of the valence d-orbital subshell is a defining feature of the transition metals and is responsible for many idiosyncratic properties of these elements, not least their propensity for forming metal−metal bonds with bond orders which are often highly sensitive to the associated ligand field. The study of dinuclear or polynuclear transition metal complexes, in which the interactions between neighboring metal atoms may fall anywhere upon a continuum ranging from multiple metal−metal bonding to weak magnetic coupling, has been one mainstay of inorganic chemistry research for the past several decades,[1,2] and an almost innumerable collection of such complexes has now been catalogued. Among very many possible representations of the versatility of metal−metal bonding motifs, our own research[3−7] has focused on understanding the properties of face-shared nonahalide dinuclear complexes ("dimers") $M_2X_9^{n-}$, which demonstrate (in miniature) the full gamut of possible intermetallic interactions within the d^3d^3 nonachloride dimers $Cr_2Cl_9^{3-}$, $Mo_2Cl_9^{3-}$, and $W_2Cl_9^{3-}$ which can be

* To whom correspondence should be addressed. E-mail: rob.stranger@anu.edu.au.

(1) Cotton, F. A.; Walton, R. A. *Multiple Bonds between Metal Atoms*, 2nd ed.; Clarendon Press: Oxford, 1993.
(2) Cotton, F. A. *Inorg. Chem.* **1998**, *37*, 5710−5720.
(3) Lovell, T.; McGrady, J. E.; Stranger, R.; Macgregor, S. A. *Inorg. Chem.* **1996**, *35*, 3079−3080.
(4) McGrady, J. E.; Lovell, T.; Stranger, R. *Inorg. Chem.* **1997**, *36*, 3242−3247.
(5) McGrady, J. E.; Stranger, R.; Lovell, T. *J. Phys. Chem. A* **1997**, *101*, 6265−6272.
(6) McGrady, J. E.; Stranger, R.; Lovell, T. *Inorg. Chem.* **1998**, *37*, 3802−3808.
(7) Stranger, R.; Turner, A.; Delfs, C. D. *Inorg. Chem.* **2001**, *40*, 4093.

10.1021/ic034525e CCC: $27.50
Published on Web 03/23/2004

rather crudely described as, respectively, weakly coupled (r(Cr−Cr) = 3.10−3.22 Å),[8−19] singly bonded (r(Mo−Mo) = 2.52−2.82 Å),[20−31] and triply bonded (r(W−W) = 2.42−2.50 Å).[13,32−44] While a satisfactory qualitative rationalization of this trend, and of many other tendencies within dinuclear or polynuclear complexes, is afforded by consideration of the influence of d-orbital dilation on the spin polarization stabilization energy and on the effectiveness of overlap between d-orbitals on adjacent metal atoms, the prediction of metal−metal bonding properties remains a rather imprecise science. Nevertheless, the theoretical investigation of as-yet-unseen dinuclear and polynuclear transition metal complexes is a very valuable complementary activity to the work of experimentalists and has the potential to greatly assist in our comprehension and quantification of the various factors impinging on metal−metal bonding properties.

Quantum chemical computation is the most sophisticated tool available to theoreticians concerned with metal−metal bonding in dinuclear or polynuclear transition metal complexes. Calculations, employing density functional theory (DFT), Hartree−Fock, or post-self-consistent-field ("post-SCF", or correlated) methodologies, have shed considerable light on the electronic factors which influence bond formation versus localization of unpaired d-electron spin density in such complexes,[3−5,45−49] while the accuracy of DFT methods in calculating optimized geometries, and vibrational frequencies, of strongly multiply bonded dinuclear complexes has been highlighted in the work of Cotton and Feng.[50,51] Considerable ongoing research activity in this field is concerned with the application of DFT or hybrid DFT methods to the structure and/or electronic configuration of dinuclear complexes. DFT has already established itself as the computational tool of choice for the study of "monomeric" transition-metal-containing complexes,[46,47,52−56] and the extension of such economical, and generally reliable, techniques to the treatment of metal complex "dimers" is a natural development in which there has been significant activity over the past decade.[3,50,51,57,58] Nevertheless, while DFT is now widely accepted as a valuable technique in inorganic chemistry, an important question remains: which density functional is best? For main-group compounds, it is generally regarded that the best performance is delivered by "hybrid DFT" techniques such as B3-LYP,[59−63] but the situation is more obscure when transition metal (TM) atoms are involved, resulting in a tendency to prefer one functional over another depending on the perceived class of compound. Despite several comparative studies of different functionals for particular chemical systems,[57,64−66] there remains no clear consensus on the appropriate DFT methodology to use in problems of TM chemistry, and in the absence of consensus much "folklore" has arisen. While the present study cannot pretend to totally redress this situation (indeed, we shall consider our task half-fulfilled if we have not merely added to the existing DFT folklore), we feel that a somewhat vexatious issue in theoretical transition-metal chemistry warrants renewed and serious attention. This issue is the description

(8) Wessel, G. J.; Ijdo, D. J. W. *Acta Crystallogr.* **1957**, *10*, 466.
(9) Earnshaw, A.; Lewis, J. **1961**, 396.
(10) Cotton, F. A. *Rev. Pure Appl. Chem.* **1967**, *17*, 25.
(11) Saillant, R.; Wentworth, R. A. D. *Inorg. Chem.* **1968**, *7*, 1606.
(12) Boyd, P. D. W.; Smith, P. W.; Wedd, A. G. *Aust. J. Chem.* **1969**, *22*, 653.
(13) Ziegler, T.; Risen, W. M., Jr. *Inorg. Chem.* **1972**, *11*, 2796.
(14) Beswick, J. R.; Dugdale, D. E. *J. Phys. C: Solid State Phys.* **1973**, *6*, 3326.
(15) Korol'kov, D. V.; Missner, K. *Teor. Eksp. Khim.* **1973**, *9*, 336.
(16) Kahn, O.; Briat, B. *Chem. Phys. Lett.* **1975**, *32*, 376.
(17) Dubicki, L.; Tanabe, Y. *Mol. Phys.* **1977**, *34*, 1531.
(18) Barry, K. R.; Maxwell, K. J.; Siddiqui, K. A.; Stevens, K. W. H. *J. Phys. C: Solid State Phys.* **1981**, *14*, 1281.
(19) Leuenberger, B.; Guedel, H. U. *Inorg. Chem.* **1986**, *25*, 181−184.
(20) Edwards, A. J.; Peacock, R. D.; Said, A. *J. Chem. Soc.* **1962**, 4643.
(21) Saillant, R.; Wentworth, R. A. D. *Inorg. Chem.* **1969**, *8*, 1226.
(22) Saillant, R.; Jackson, R. B.; Streib, W.; Folting, K.; Wentworth, R. A. D. *Inorg. Chem.* **1971**, *10*, 1453.
(23) Subbotin, M. Y.; Aslanov, L. A. *Zh. Neorg. Khim.* **1985**, *30*, 1431.
(24) Subbotin, M. Y.; Kazin, P. E.; Aslanov, L. A.; Zelentsov, V. V. *Koord. Khim.* **1985**, *11*, 1568.
(25) Smith, P. W.; Stranger, R. *Aust. J. Chem.* **1986**, *39*, 1269.
(26) Spitsyn, V. I.; Kazin, P. E.; Subbotin, M. Y.; Aslanov, L. A.; Zelentsov, V. V.; Zhirov, A. I.; Felin, M. G. *Dokl. Akad. Nauk SSSR* **1986**, *287*, 134.
(27) Spitsyn, V. I.; Kazin, P. E.; Subbotin, M. Y.; Aslanov, L. A.; Zhirov, A. I.; Zelentsov, V. V.; Felin, M. G. *Koord. Khim.* **1986**, *12*, 1563.
(28) Subbotin, M. Y.; Aslanov, L. A. *Zh. Neorg. Khim.* **1986**, *31*, 393.
(29) Subbotin, M. Y.; Aslanov, L. A. *Zh. Neorg. Khim.* **1986**, *31*, 901.
(30) Stranger, R.; Grey, I. E.; Madsen, I. C.; Smith, P. W. *J. Solid State Chem.* **1987**, *69*, 162.
(31) Stranger, R.; Smith, P. W.; Grey, I. E. *Inorg. Chem.* **1989**, *28*, 1271.
(32) Collenberg, O.; Sandved, K. *Z. Anorg. Allg. Chem.* **1923**, *130*, 1.
(33) Brosset, C. *Nature* **1935**, *135*, 874.
(34) Klemm, W.; Steingberg, H. *Z. Anorg. Allg. Chem.* **1936**, *227*, 193.
(35) Watson, W. H., Jr.; Waser, J. *Acta Crystallogr.* **1958**, *11*, 689.
(36) Saillant, R.; Hayden, J. L.; Wentworth, R. A. D. *Inorg. Chem.* **1967**, *6*, 1497.
(37) Hayden, J. L.; Wentworth, R. A. D. *J. Am. Chem. Soc.* **1968**, *90*, 5291.
(38) Lewis, J.; Nyholm, R. S.; Smith, P. W. *J. Chem. Soc. A* **1969**, 57.
(39) Saillant, R.; Wentworth, R. A. D. *J. Am. Chem. Soc.* **1969**, *91*, 2174.
(40) Smith, P. W.; Wedd, A. G. *J. Chem. Soc. A* **1970**, 2447.
(41) Clark, P. W.; Wentworth, R. A. D. *Inorg. Chem.* **1969**, *8*, 1223.
(42) Trogler, W. C. *Inorg. Chem.* **1980**, *19*, 697.
(43) Scheffler, T. B.; Hussey, C. L. *Inorg. Chem.* **1984**, *23*, 1926.
(44) Dunbar, K. R.; Pence, L. E. *Acta Crystallogr.* **1991**, *C47*, 23.
(45) Bursten, B. E.; Clark, D. L. *Polyhedron* **1987**, *6*, 695.
(46) Hall, M. B. *Polyhedron* **1987**, *6*, 679.
(47) Ziegler, T.; Tschinke, V.; Becke, A. D. *Polyhedron* **1987**, *6*, 685.
(48) Andersson, K.; Bauschlicher, C. W., Jr.; Persson, B. J.; Roos, B. O. *Chem. Phys. Lett.* **1996**, *257*, 238.
(49) Cotton, F. A.; Feng, X. *Int. J. Quantum Chem.* **1996**, *58*, 671.
(50) Cotton, F. A.; Feng, X. *J. Am. Chem. Soc.* **1997**, *119*, 7514.
(51) Cotton, F. A.; Feng, X. *J. Am. Chem. Soc.* **1998**, *120*, 3387.
(52) Deeth, R. J. In *Coordination Chemistry*; 1995; Vol. 82, p 1.
(53) Laird, B. B.; Ross, R. P.; Ziegler, T. In *Chemical Applications of Density-Functional Theory*; 1996; Vol. 629, p 1.
(54) Chermette, H. *Coord. Chem. Rev.* **1998**, *180*, 699.
(55) Velde, G. T.; Bickelhaupt, F. M.; Baerends, E. J.; Guerra, C. F.; van Gisbergen, S. J. A.; Snijders, J. G.; Ziegler, T. *J. Comput. Chem.* **2001**, *22*, 931.
(56) Ziegler, T. *J. Chem. Soc., Dalton Trans.* **2002**, 642.
(57) Barden, C. J.; Rienstra-Kiracofe, J. C.; Schaefer, H. F. *J. Chem. Phys.* **2000**, *113*, 690.
(58) Bridgeman, A. J.; Cavigliasso, G. *J. Phys. Chem. A* **2001**, *105*, 7111.
(59) Raghavachari, K.; Stefanov, B. B.; Curtiss, L. A. *Mol. Phys.* **1997**, *91*, 555.
(60) Curtiss, L. A.; Raghavachari, K.; Redfern, P. C.; Pople, J. A. *J. Chem. Phys.* **1997**, *106*, 1063.
(61) Redfern, P. C.; Blaudeau, J. P.; Curtiss, L. A. *J. Phys. Chem. A* **1997**, *101*, 8701.
(62) Martell, J. M.; Goddard, J. D.; Eriksson, L. A. *J. Phys. Chem. A* **1997**, *101*, 1927.
(63) Scheiner, A. C.; Baker, J.; Andzelm, J. W. *J. Comput. Chem.* **1997**, *18*, 775.
(64) Eriksson, L. A.; Pettersson, L. G. M.; Siegbahn, P. E. M.; Wahlgren, U. *J. Chem. Phys.* **1995**, *102*, 872.
(65) Siegbahn, P. E. M.; Blomberg, M. R. A. *Annu. Rev. Phys. Chem.* **1999**, *50*, 221.
(66) Yanagisawa, S.; Tsuneda, T.; Hirao, K. *J. Chem. Phys.* **2000**, *112*, 545.

by DFT of the competition between bonding and nonbonding interactions between two (or more) TM atoms, in oligonuclear TM complexes.

Just why is the treatment of the metal−metal bond, by quantum chemical methods which have otherwise enjoyed a prolonged and very considerable degree of success in solving structural, thermochemical, and electronic problems, so awkward? One important reason is that in many cases the π- and δ-type interactions involved are weak, and when accompanied by inefficient σ-overlap, the direct metal−metal bond is sometimes a rather fragile thing. In such comparatively weakly bonded dimeric complexes as, for example, $Mo_2Cl_9^{3-}$, the choice of one functional over another can drastically influence the calculated metal−metal bond length. For $Mo_2Cl_9^{3-}$, for which crystallographic values of the Mo−Mo bond length range from 2.52 to 2.82 Å,[22,24,28,30,31] ostensibly sensible DFT approaches deliver values which vary from 2.29 to 3.45 Å.[3,5] Such a dramatic variation in distances, seen in both the experimental and theoretical results, is symptomatic of a very shallow and broad bonding region of the potential energy surface. While none of the DFT methods explored to date has delivered a Mo−Mo distance in precise accord with experiment, better agreement, diagnosed both by the closeness of the calculated bond length to the literature values, and by the shallowness of the potential energy surface over the Mo−Mo range of interest, is shown by the local-density-approximation (LDA) than by more sophisticated gradient-corrected methods such as Perdew−Wang (PW) and Becke−Perdew (BP).[5]

In the present work, the complexes surveyed are structurally diverse, in that TM oxidation states, TM valence d-orbital occupations, ligands, bridging modes, and overall charge states all vary substantially within our selected "test set". Complexes in this "test set", which are either experimentally well-characterized species (for which crystallographic geometries have been reported) or are close analogues of such species, have been selected to encompass a spectrum of metal−metal interactions ranging from weak coupling to multiple bonding. As in previous studies, we have employed the broken-symmetry (BS) technique[67−69] in density functional theory (DFT) calculations on the bimetallic complexes of interest. The broken-symmetry approach, which introduces an asymmetry in the initial spin densities on the two metal atoms, allows variation of the metal−metal bond order along a continuum ranging from weak antiferromagnetic coupling to strong multiple metal−metal bond formation. We have previously found the BS method, employed (as here) in spin-unrestricted calculations, to be particularly useful in elucidating the degree of metal−metal bonding in various face-shared and edge-shared dinuclear complexes,[3−6] and the more general applicability and utility of this approach has been highlighted in a recent review.[69]

Computational Details

Unless otherwise indicated, all calculations described in this work were performed on Linux-based Pentium IV 1.7−2.8 GHz computers using the Amsterdam Density Functional (ADF) program, version ADF2002.03,[70] developed by Baerends et al.[71] Basis sets used in all calculations were of triple-ζ quality including polarization functions (TZP) with frozen core sizes as specified within the text for each complex. All calculations were performed in a spin-unrestricted fashion and employed the broken symmetry (BS) technique.

Optimized geometries were obtained using the gradient algorithm of Versluis and Ziegler.[72] Potential energy curves for the BS state were obtained for each dimer by optimization of all other structural parameters along a series of fixed metal−metal distances. Scalar relativistic corrections, when included, were obtained with the ZORA (zero order regular approximation) formalism[73,74] using basis sets and frozen cores analogous to those used in the uncorrected calculations. Density functionals used in geometry optimization and frequency calculations were (individually or in combination) the Xα and Vosko−Wilk−Nusair (VWN)[75] parametrizations of electron gas in the local density approximation (LDA); the Becke-Lee−Yang−Parr (B-LYP)[76,77] combination of exchange and correlation nonlocal corrections, implemented with either the Xα or the VWN local functional; the Perdew−Wang (PW91),[78] Becke−Perdew (BP),[76,79] and Perdew−Burke−Ernzerhof (PBE)[80] combined exchange/correlation nonlocal corrections; and two additional variants of the PBE nonlocal functional, the nonlocal-exchange modifications of Hammer et al. (RPBE)[81] and Zhang and Wang (revPBE).[82]

In the discussion which follows, we distinguish explicitly between B-LYP (which, in its orthodox fomulation, includes the Xα treatment of local density)[77] and VWN+B-LYP. Note, however, that all other "gradient-corrected" methods used here (viz., BP, PW91, PBE, RPBE, and revPBE), implicitly use the VWN functional rather than Xα.

For the case of $Mo_2Cl_9^{3-}$ only, additional B-LYP and B3-LYP optimizations were performed using the GAUSSIAN98 program suite.[83] These calculations, also featuring broken symmetry, used the SDD (Stuttgart/Dresden relativistic ECP) basis set.[84]

(67) Noodleman, L.; Norman, J. G., Jr. *J. Chem. Phys.* **1979**, *70*, 4903.
(68) Noodleman, L. *J. Chem. Phys.* **1981**, *74*, 5737.
(69) Ruiz, E.; Cano, J.; Alvarez, S.; Alemany, P. *J. Comput. Chem.* **1999**, *20*, 1391.
(70) Baerends, E. J.; Bérces, A.; Bo, C.; Boerrigter, P. M.; Cavallo, L.; Deng, L.; Dickson, R. M.; Ellis, D. E.; Fan, L.; Fischer, T. H.; Fonseca Guerra, C.; van Gisbergen, S. J. A.; Groeneveld, J. A.; Gritsenko, O. V.; Harris, F. E.; van den Hoek, P.; Jacobsen, H.; van Kessel, G.; Kootstra, F.; van Lenthe, E.; Osinga, V. P.; Philipsen, P. H. T.; Post, D.; Pye, C.; Ravenek, W.; Ros, P.; Schipper, P. R. T.; Schreckenbach, G.; Snijders, J. G.; Sola, M.; Swerhone, D.; te Velde, G.; Vernooijs, P.; Versluis, L.; Visser, O.; van Wezenbeek, E.; Wiesenekker, G.; Wolff, S. K.; Woo, T. K.; Ziegler, T. *ADF2002.03*; S.C.M., Vrije Universiteit, Theoretical Chemistry: Amsterdam, The Netherlands, 2002.
(71) Fonseca Guerra, C.; Snijders, J. G.; te Velde, G.; Baerends, E. J. *Theor. Chem. Acc.* **1998**, *99*, 391−403.
(72) Versluis, L.; Ziegler, T. J. *J. Chem. Phys.* **1988**, *88*, 322−328.
(73) van Lenthe, E.; Baerends, E. J.; Snijders, J. G. *J. Chem. Phys.* **1993**, *99*, 4597.
(74) van Lenthe, E.; Ehlers, A. E.; Baerends, E. J. *J. Chem. Phys.* **1999**, *110*, 8943.
(75) Vosko, S. H.; Wilk, L.; Nusair, M. *Can. J. Phys.* **1980**, *58*, 1200.
(76) Becke, A. D. *Phys. Rev. A* **1988**, *38*, 3098.
(77) Lee, C.; Yang, W.; Parr, R. G. *Phys. Rev. B* **1988**, *37*, 785.
(78) Perdew, J. P.; Chevary, J. A.; Vosko, S. H.; Jackson, K. A.; Pederson, M. R.; Singh, D. J.; Fiolhais, C. *Phys. Rev. B.* **1992**, *46*, 6671.
(79) Perdew, J. P. *Phys. Rev. B* **1986**, *33*, 8822.
(80) Perdew, J. P.; Burke, K.; Ernzerhof, M. *Phys. Rev. Lett.* **1996**, *77*, 3865.
(81) Hammer, B.; Hansen, L. B.; Norskov, J. K. *Phys. Rev. B* **1999**, *59*, 7413.
(82) Zhang, Y.; Yang, W. *Phys. Rev. Lett.* **1998**, *80*, 890.

Table 1. Optimized Metal−Metal Distances Obtained for Neutral and Singly charged Dinuclear Complexes

species	structural motif[a]	r(M−M)[b]/Å									
		expt[c]	VWN	VB[d]	PW91	PBE	BP	Xα	revPBE	RPBE	B-LYP
$Zr_2(PH_3)_4I_6$	ES	3.39	3.325	3.489	*3.401*	*3.401*	*3.427*	*3.398*	*3.422*	*3.410*	3.548
$V_2Cl_3(O(CH_3)_2)_6^+$	FS	2.97−3.02	2.814	*2.980*	*3.036*	3.059	3.076	3.054	3.117	3.155	3.121
$Cr_2(O_2CH)_4$	PW	1.97−2.29?	1.796	1.809	*1.995*	*1.996*	*2.003*	*2.244*	*2.257*	*2.295*	*2.085*
$Cr_2(O_2CCH_3)_4$	PW	1.97−2.29	1.787	1.803	1.895	1.895	1.902	*2.101*	1.938	*2.225*	*1.964*
$Mo_2(H_2PCH_2PH_2)_2Cl_6$	ES	2.73−2.83	2.682	*2.742*	*2.818*	*2.821*	2.861	*2.796*	2.881	2.908	2.947
$Mo_2(NH_2)_6$	NB	2.21	*2.200*	*2.226*	*2.228*	*2.228*	*2.230*	*2.235*	*2.235*	*2.237*	*2.259*
$Re_2Cl_9^-$	FS	2.70−2.73	*2.718*	2.871	2.948	2.954	3.013	2.895	3.282	3.322	3.392
$Rh_2(O_2CCH_3)_4(CO)_2$	PW	2.42	2.483	2.495	2.502	2.507	2.502	2.519	2.517	2.514	2.528

[a] ES = edge-shared bioctahedral complex; FS = face-shared bioctahedral complex; PW = paddlewheel (tetracarboxylate) complex; NB = nonbridged complex. [b] Optimized metal−metal separation according to the indicated method. All calculations were performed with TZP basis sets, using the broken-symmetry technique of Noodleman and Norman (ref 67). [c] M−M distance range embodied in previously reported crystallographic studies, as identified within the text for each complex. [d] VB = VWN+B-LYP (see text for details).

Finally, $V_2Cl_3(dme)_6^+$, $Mo_2(H_2PCH_2PH_2)_2Cl_6$, and $Mo_2Cl_9^{3-}$ were employed in calculations designed to assess the expected performance of several "meta-GGA" functionals recently incorporated into the ADF code.[55] The latter methods are currently available only for single-point calculations, but an estimation of their geometry optimization tendencies was made through execution of a sequence of single-point calculations employing partially optimized geometries obtained through linear-transit calculations with incrementally varied intermetallic distances.

Results and Discussion

For purposes of structural organization, we have partitioned our discussion of results into subsections dealing in turn with (i) neutral or singly charged and (ii) multiply charged dinuclear complexes. Following an assessment of the computational performance for each of the modeled dimers within each subsection, we present an overall analysis of our results.

1. Neutral and Singly Charged Dinuclear Complexes. Results of geometry optimizations for the complexes within this category are presented in Table 1. To illustrate the performance of each DFT method for each of these complexes, optimized metal−metal bond lengths in this table are italicized if they fall within the "target range", which we define as the larger of (i) the range of experimentally observed bond lengths for a given complex, or (ii) $r_{mid} \pm 0.05$ Å, where r_{mid} is the midpoint of the experimental M−M bond length range. The DFT methods represented in Table 1 are ranked in approximate order of their tendency to deliver progressively increasing metal−metal bond lengths. Geometry optimizations were performed, in the default case, without consideration of relativistic effects. For some species, as detailed in subsection 1.9, optimizations were also undertaken using the ZORA formalism to apply scalar relativistic corrections.

1.1. $Zr_2(PH_3)_4I_6$. This phosphine-containing compound is a close analogue of the species $Zr_2(PMe_3)_4I_6$ and $Zr_2(PMe_2Ph)_4I_6$ which have been characterized in the laboratory,[85] and previous calculations on $Zr_2(PH_3)_4I_6$, using the Fenske−Hall molecular orbital treatment, have been used to analyze the bonding tendencies in the larger trimethylphosphine- and dimethylphenylphosphine-containing complexes.[85] The X = Cl and X = Br forms of the structure $Zr_2(PMe_3)_4X_6$ are also known.[86,87] For the two (μ-I)$_2$ structures known, Zr−Zr bond lengths of 3.39 and 3.44 Å have been reported, apparently indicating a long but essentially intact single bond between zirconium atoms.[85]

All of the orthodox gradient-corrected functionals tested, except for B-LYP, yield Zr−Zr bond length values within the target range, as does Xα. Both B-LYP and the VWN+B-LYP variant overestimate r(Zr−Zr): as will be seen, this is rather more typical of B-LYP than of VWN+B-LYP. Also typical is the underestimation by VWN, often criticized as an "overbinding" technique prone to calculation of bond lengths which are markedly too short.

1.2. $V_2Cl_3(O(CH_3)_2)_6^+$. This tri-μ-chloro complex is closely analogous to the $V_2Cl_3(OR_2)_6^+$ ion (OR_2 = THF, 3-methyltetrahydrofuran) for which crystal structures with several different counterions have been reported.[88−92] V−V bond lengths in all instances were found to fall in the range 2.97−3.02 Å. A similar V−V separation is also found when the O-donor ligands are replaced wholesale by PMe_3,[93] and so, it is reasonable to expect that the substitution in our calculations of dimethyl ether for tetrahydrofuran, for reasons

(83) Frisch, M. J.; Trucks, G. W.; Schlegel, H. B.; Scuseria, G. E.; Robb, M. A.; Cheeseman, J. R.; Zakrzewski, V. G.; Montgomery, J. A., Jr.; Stratmann, R. E.; Burant, J. C.; Dapprich, S.; Millam, J. M.; Daniels, A. D.; Kudin, K. N.; Strain, M. C.; Farkas, O.; Tomasi, J.; Barone, V.; Cossi, M.; Cammi, R.; Mennucci, B.; Pomelli, C.; Adamo, C.; Clifford, S.; Ochterski, J.; Petersson, G. A.; Ayala, P. Y.; Cui, Q.; Morokuma, K.; Malick, D. K.; Rabuck, A. D.; Raghavachari, K.; Foresman, J. B.; Cioslowski, J.; Ortiz, J. V.; Stefanov, B. B.; Liu, G.; Liashenko, A.; Piskorz, P.; Komaromi, I.; Gomperts, R.; Martin, R. L.; Fox, D. J.; Keith, T.; Al-Laham, M. A.; Peng, C. Y.; Nanayakkara, A.; Gonzalez, C.; Challacombe, M.; Gill, P. M. W.; Johnson, B. G.; Chen, W.; Wong, M. W.; Andres, J. L.; Head-Gordon, M.; Replogle, E. S.; Pople, J. A. *Gaussian 98*; Gaussian, Inc.: Pittsburgh, PA, 1998.
(84) Bergner, A.; Dolg, M.; Kuechle, W.; Stoll, H.; Preuss, H. *Mol. Phys.* **1993**, *80*, 1431.
(85) Cotton, F. A.; Shang, M.; Wojtczak, W. A. *Inorg. Chem.* **1991**, *30*, 3670.
(86) Cotton, F. A.; Wojtczak, W. A. *Gazz. Chim. Ital.* **1993**, *123*, 499.
(87) Troyanov, S. I.; Meetsma, A.; Teuben, J. H. *Inorg. Chim. Acta* **1998**, *271*, 180.
(88) Bouma, R. J.; Teuben, J. H.; Beukema, W. R.; Bansemer, R. L.; Huffman, J. C.; Caulton, K. G. *Inorg. Chem.* **1984**, *23*, 2715.
(89) Cotton, F. A.; Duraj, S. A.; Roth, W. J. *Inorg. Chem.* **1985**, *24*, 913.
(90) Canich, J. A. M.; Cotton, F. A.; Duraj, S. A.; Roth, W. J. *Polyhedron* **1987**, *6*, 1433.
(91) Calderazzo, F.; De Benedetto, G. E.; Pampaloni, G.; Mossmer, C. M.; Strahle, J.; Wurst, K. *J. Organomet. Chem.* **1993**, *451*, 73.
(92) Pampaloni, G.; Engert, U. *Inorg. Chim. Acta* **1995**, *231*, 167.
(93) Cotton, F. A.; Duraj, S. A.; Manzer, L. E.; Roth, W. J. *J. Am. Chem. Soc.* **1985**, *107*, 3850.

of computational expediency, should not significantly affect the calculated bond lengths of interest.

As a d^3d^3 face-shared dinuclear complex, with a bridging mode seen in other instances to accommodate triply bonded, singly bonded, or effectively nonbonded metal atoms, this vanadium dimer represents a more challenging species than edge-shared $Zr_2(PH_3)_4I_6$, and fewer "direct hits" are seen among our selection of DFT methods. Nevertheless, our computed values using VWN+B-LYP and PW91 are within the target range, while PBE, BP, and Xα also perform quite well. Again, B-LYP delivers an exaggerated M−M bond length (joined by RPBE and revPBE), and VWN falls short.[94]

1.3. $Cr_2(O_2CH)_4$. An extensive compilation of theoretical results[48,99−108] has already been reported for $Cr_2(O_2CH)_4$ which is, as yet, not characterized experimentally: comparison of the results of Andersson et al.[48] for the tetraformate and tetraacetate species (see below), using the same DFT methods for each, suggests that dichromium tetraformate should possess a Cr−Cr separation of 2.0 Å or less in the gas phase. Computational methods which have yielded such a short bond length for $Cr_2(O_2CH)_4$ include Xα (1.87 Å)[105] and RB3-LYP (1.808 Å),[48] while bond lengths of 2.3 Å or larger have been returned by CI (2.53 Å[103] and 2.41 Å),[106] GVB (2.49 Å),[108] UB-LYP (2.32 Å, but with some dependence on basis set evident),[48] UB3-LYP (2.62−2.63 Å),[48] CASSCF (2.853 Å),[48] and CASPT2 (2.544 Å).[48]

While the performance of different theoretical approaches for this complex is a topic of some interest (not least because of the wide variety of previous calculated results with which to draw comparisons), there is little which can safely be inferred in terms of the relative reliability of the methods surveyed here, because of the extreme variability in Cr−Cr bond lengths in this class of complex. We can note that all of the orthodox gradient-corrected methods, and Xα, return results within the target range (which equates with that ascribed to the analogous tetraacetate complex, see below); while VWN and VWN+B-LYP deliver comparatively small Cr−Cr separations, there are no methods among those surveyed here which give bond lengths larger than those of the target range. Thus, the trend evident from our results is suggestive of the short Cr−Cr bond exhibited within the gas-phase diffraction study of the tetraformate complex (see below), rather than the longer bond seen in the crystalline state. Nevertheless, most methods predict (see Figure 1) a notably flattened potential energy surface across the target range (VWN and VWN+B-LYP are clear exceptions). The PES graph depicted in Figure 1 highlights not only the considerable variation in optimized M−M distance minima, but also the very clear "overbinding" tendency of VWN and of VWN+B-LYP.

1.4. $Cr_2(O_2CCH_3)_4$. The "bare" $Cr_2(OAc)_4$ molecule has been structurally characterized both in the gas phase, for which an electron diffraction study[109] yielded a Cr−Cr value of 1.966 Å, and in the solid state (using crystals obtained by vacuum sublimation) for which a Cr−Cr distance of 2.288 Å was obtained.[110] The very large difference between the gas-phase and crystalline bond lengths is ascribed to the tendency toward infinite chain formation in the solid state, and this sensitivity of the Cr−Cr bond to axial coordination can be seen also in the (axially hydrated) crystal structure result for $Cr_2(OAc)_4(OH_2)_2$ of 2.362 Å.[111] The only other dichromium tetracarboxylate complex yet isolated without axial ligands is the analogous compound $Cr_2(O_2CCMe_3)_4$,[112,113] for which r(Cr−Cr) = 2.388 Å was found.[112] While the electron diffraction measurement[109] appears to represent the shortest Cr−Cr bond in a tetracarboxylate complex, values in excess of 2.5 Å have been noted at the other extreme,[1] and this has led to speculation that the typical PES for such compounds features a very broad and shallow region around the minimum-energy configuration.[112]

The only electronic structure calculations on $Cr_2(OAc)_4$ to have been reported are those of Andersson et al.,[48] who employed DFT (restricted (R) and unrestricted (U) B3-LYP, and UB-LYP with various basis sets). Notably, all of these methods except RB3-LYP (in which fully quadruple Cr−Cr bond formation is enforced as a consequence of molecular and α,β-orbital symmetry) predicted[48] Cr−Cr distances markedly in excess of the crystallographically derived value, and 0.4−0.6 Å larger than the experimental gas-phase value. Since calculations on electrically neutral vacuum-phase

(94) We have attempted also to assess the relative performances of several "meta-generalized-gradient-approximation" (meta-GGA) methods which are now available for single-point calculations within the ADF2002 program suite.[70] To perform this evaluation, we obtained partially optimized geometries for $V_2Cl_3(O(CH_3)_2)_6^+$ as a function of V−V distance from a linear transit calculation using the PBE functional.[80] The PBE functional was then also used to define the exchange/correlation (xc) potential for the subsequent meta-GGA single-point calculations. The effective potential energy scans which resulted allowed identification of several meta-GGA methods whose performance for this species appeared promising: Filatov-Thiel 98[95] (FT98; V−V ∼ 2.93 Å), Krieger−Chen−Iafrate−Savin[96] (KCIS; V−V ∼ 2.96 Å), the combination of Perdew−Kurth−Zupan−Blaha exchange[97,98] and KCIS correlation[96] (PKZBx-KCIScor; V−V ∼ 2.99 Å), and the (unpublished) modified KCIS energy functional (modKCIS; V−V ∼ 3.02 Å). Several other meta-GGAs delivered apparently poorer performance in this instance, with V−V separations between 3.13 and 3.20 Å representing a significant overestimation of the experimental metal−metal distance.

(95) Filatov, M.; Thiel, W. *Phys. Rev. A* **1998**, *57*, 189.
(96) Krieger, J. B.; Chen, J.; Iafrate, G. J.; Savin, A. In *Electron Correlation and Materials Properties*; Gonis, A., Kioussis, N., Eds.; Plenum: New York, 1999.
(97) Perdew, J. P.; Kurth, S.; Zupan, A.; Blaha, P. *Phys. Rev. Lett.* **1999**, *82*, 2544.
(98) Perdew, J. P.; Kurth, S.; Zupan, A.; Blaha, P. *Phys. Rev. Lett.* **1999**, *82*, 5179.
(99) Benard, M. *J. Am. Chem. Soc.* **1978**, *100*, 2354.
(100) Benard, M. *J. Chem. Phys.* **1979**, *71*, 2546.
(101) Atha, P. M.; Hillier, I. H.; Guest, M. F. *Mol. Phys.* **1982**, *46*, 437.
(102) Atha, P. M.; Campbell, J. C.; Garner, C. D.; Hillier, I. H.; Macdowell, A. A. *J. Chem. Soc., Dalton Trans.* **1983**, 1085.
(103) Wiest, R.; Benard, M. *Chem. Phys. Lett.* **1983**, *98*, 102.
(104) Kok, R. A.; Hall, M. B. *J. Am. Chem. Soc.* **1983**, *105*, 676.
(105) Ziegler, T. *J. Am. Chem. Soc.* **1985**, *107*, 4453.
(106) Kok, R. A.; Hall, M. B. *Inorg. Chem.* **1985**, *24*, 1542.
(107) Cotton, F. A.; Feng, X.; Kibala, P. A.; Matusz, M. *J. Am. Chem. Soc.* **1988**, *110*, 2807.
(108) Davy, R. D.; Hall, M. B. *J. Am. Chem. Soc.* **1989**, *111*, 1268.
(109) Kektar, S. N.; Fink, M. *J. Am. Chem. Soc.* **1985**, *107*, 338.
(110) Cotton, F. A.; Rice, C. E.; Rice, G. W. *J. Am. Chem. Soc.* **1977**, *99*, 4704.
(111) Cotton, F. A.; DeBoer, B. G.; LaPrade, M. D.; Pipal, J. R.; Ucko, D. A. *Acta Crystallogr.* **1971**, *B27*, 1664.
(112) Cotton, F. A.; Extine, M. W.; Rice, G. W. *Inorg. Chem.* **1978**, *17*, 176.
(113) Bennes, L.; Kalousova, J.; Votinsky, J. *J. Organomet. Chem.* **1985**, *290*, 147.

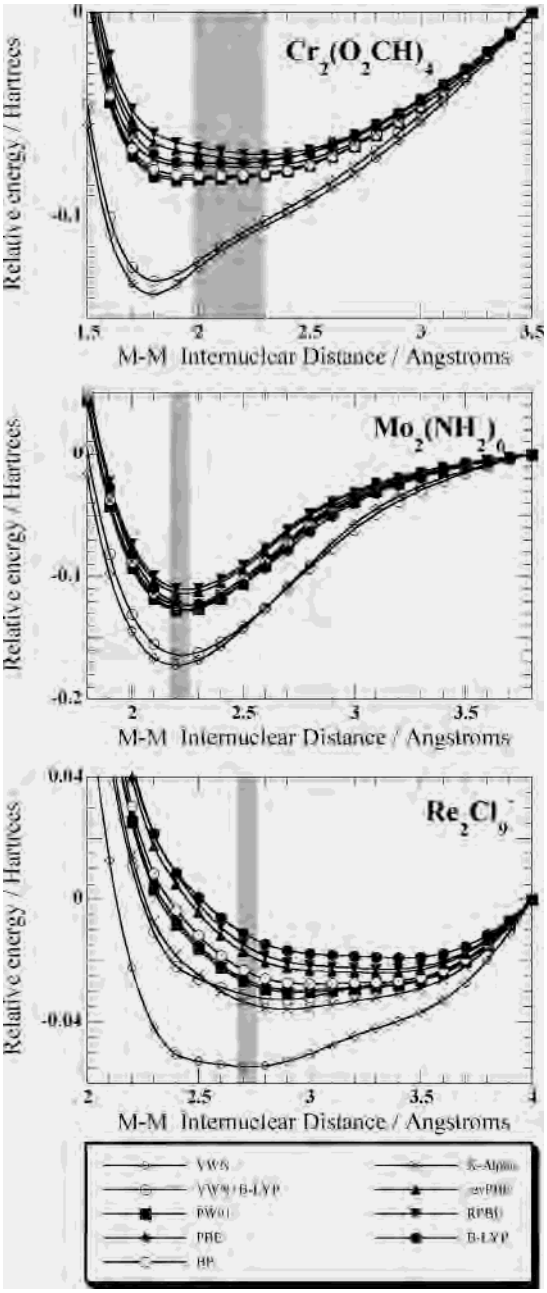

Figure 1. Potential energy curves, obtained using the broken-symmetry (BS) technique and the indicated density functional methodology, for the dinuclear complexes $Cr_2(O_2CH)_4$, $Mo_2(NH_2)_6$, and $Re_2Cl_9^-$. To facilitate comparison of the performance of different functionals, energy values for all functionals are expressed relative to the total energy of the partially optimized structure at the largest modeled M−M separation, while the "target range" encompassing the experimentally observed range of M−M distances (as defined in the text) is shown in gray.

structures should more closely adhere to gas-phase geometries than to the "distortions" induced by crystallization, the results of Andersson et al.[48] suggest poor performance by the techniques employed in that study. However, it should also be remembered that DFT calculations on dinuclear transition-metal complexes are usually undertaken with the intended aim of rationalizing crystalline state, rather than gas phase, properties. In this context, the closest match seen by Andersson et al.[48] with the crystallographic Cr−Cr value of 2.29 Å was seen when UB-LYP was used, typically yielding r(Cr−Cr) = 2.40 Å with negligible dependence upon the basis set used for Cr. The hybrid functional UB3-LYP, generally regarded as being more reliable than "pure" functionals such as (U)B-LYP, performed poorly with an 0.3 Å overestimation of the crystallographic value.

In an illuminating point of comparison with the earlier study,[48] we note that most of the functionals employed in the present work gave results much closer to (and generally below) the gas-phase Cr−Cr value, suggesting that (in the case of B-LYP at least) basis set composition has a significant influence on the result. The best performances seen among the gradient-corrected methods are those of B-LYP, which skirts the lower edge of the target range, and RPBE, toward the upper end of the range: note that these two methods, for most of the other complexes to be considered in the present study, are the "worst offenders" for metal−metal bond length overestimation. A notable apparent failure of the VWN and VWN+B-LYP methods for this compound is that they exhibit a more pronounced minimum at significantly too short a Cr−Cr separation to match even the short gas-phase intermetallic distance.

1.5. $Mo_2(H_2PCH_2PH_2)_2Cl_6$. This compound shares with $Zr_2(PH_3)_4I_6$ (see above) the structural motif of halide edge-sharing, but it has equatorial coordination of the nonbridging halides, and axial bridging P-containing ligands. This species is structurally very similar to (and computationally more tractable than) the known chloride-edge-sharing, diphosphine-bridged complexes $Mo_2(Ph_2PCH_2PPh_2)_2Cl_6$,[114] $Mo_2(Me_2PCH_2PMe_2)_2Cl_6$,[115] and $Mo_2(Ph_2PCH_2PPh_2)_2Cl_4I_2$,[116] which possess Mo−Mo bonds of between 2.73 and 2.83 Å; additional analogous compounds have also been reported[116,117] but appear not to have been crystallographically characterized. Bond lengths in the same range are also generally recorded for other $Mo_2P_4Cl_6$ complexes involving unidentate,[118] bidentate,[119] or polydentate[120] phosphine ligands, despite substantial differences in the Mo coordination sites apparently preferred by different phosphines: a remarkable exception is seen in the case of $Mo_2(PEt_3)_4Cl_6$,[118,121] for which an Mo−Mo separation of 3.73 Å is found.

The gradient-corrected methods PW91 and PBE are joined by VWN+B-LYP and Xα in reaching the target range; typically, VWN underestimates while B-LYP and RPBE overestimate (as do, in this instance, revPBE and BP also).[122]

(114) Chakravarty, A. R.; Cotton, F. A.; Diebold, M. P.; Lewis, D. B.; Roth, W. J. *J. Am. Chem. Soc.* **1986**, *108*, 971.
(115) Canich, J. A. M.; Cotton, F. A.; Daniels, L. M.; Lewis, D. B. *Inorg. Chem.* **1987**, *26*, 4046.
(116) Cotton, F. A.; Daniels, L. M.; Dunbar, K. R.; Falvello, L. R.; O'Connor, C. J.; Price, A. C. *Inorg. Chem.* **1991**, *30*, 2509.
(117) Pistorio, B. J.; Nocera, D. G. *Chem. Commun.* **1999**, 1831.
(118) Poli, R.; Mui, H. D. *Inorg. Chem.* **1991**, *30*, 65.
(119) Agaskar, P. A.; Cotton, F. A.; Dunbar, K. R.; Falvello, L. R.; O'Connor, C. J. *Inorg. Chem.* **1987**, *26*, 4051.
(120) Cotton, F. A.; Hong, B.; Shang, M.; Stanley, G. G. *Inorg. Chem.* **1993**, *32*, 3620.
(121) Poli, R.; Gordon, J. C. *J. Am. Chem. Soc.* **1992**, *114*, 6723.
(122) As with $V_2Cl_3(O(CH_3)_2)_6^+$,[94] we employed the PBE functional in linear-transit calculations to assess the performance of various meta-GGA functionals for $Mo_2(H_2PCH_2PH_2)_2Cl_6$. None of the identified best-performing meta-GGAs for the vanadium complex did well in this instance, with better matches provided by Filatov−Thiel 97[123] (FT97) and Becke−Tsuneda−Suzumura−Hirao[76,124] (BOP) both yielding Mo−Mo ∼ 2.90 Å.

We have also performed relativistically corrected geometry optimizations for this species, as discussed in subsection 1.9.

1.6. $Mo_2(NH_2)_6$. Three previous DFT studies on this species have been conducted,[125−127] one of which[127] included also an investigation of the fully methylated analogue $Mo_2[N(CH_3)_2]_6$ for which a Mo−Mo bond length of 2.214 Å has been reported.[128] While none of these earlier studies featured full geometry optimizations of the $Mo_2(NH_2)_6$ structure, the partial optimizations which have been performed − using the Xα and B-LYP functionals − have both yielded bond lengths, of 2.22 and 2.256 Å, respectively,[125,126] which are in excellent agreement with the experimental value for the methylated species.

Alone among the 16 dinuclear complexes studied here, $Mo_2(NH_2)_6$ stands out as the species for which all of the DFT methods surveyed yield a metal−metal separation within the target range (see Figure 1). This observation may seem contrary to our assertion that the metal−metal interaction is particularly problematic to treat via DFT, while the more straightforward metal−ligand interaction is treated quite well: here is a compound, after all, which is held together solely by virtue of its metal−metal bonding without the assistance of any bridging metal−ligand interactions. In light of the result for $Mo_2(NH_2)_6$, it would appear that one of the most problematic aspects in the computational treatment of metal−metal interactions is in balancing the magnitude of the direct metal−metal and bridging interactions: when competition exists between the optimum intermetallic separation for metal−metal bonding (ignoring the geometric requirements of bridging ligands) and the optimum metal−metal distance for "relaxation" of the bridging ligands, there is scope for a notably broad and flat potential energy well. Such a loosely defined well is clearly evident (from the reported crystal structures, as well as from our own DFT calculations; see below) for the $Mo_2Cl_9^{3-}$ species, and it is this type of feature which is most sensitive to the limitations of existing nonlocal functionals. No such competition (between Mo−Mo bonding and bridging) exists within $Mo_2(NH_2)_6$, and hence, the potential energy well has a sharply defined (and essentially consistent) dependence on the intermetallic separation with all the functional combinations employed in this study.

We have also performed relativistically corrected geometry optimizations for this species, as discussed in subsection 1.9.

1.7. $Re_2Cl_9^-$. The nonachlorodirhenate(IV) ion, which like $V_2Cl_3(O(CH_3)_2)_6^+$ has a d^3d^3 valence electron configuration, was first isolated in solution and in the solid state in the company of the tetrabutylammonium counterion.[129] Subsequent characterization of the crystal structures of this compound,[130] and of analogous compounds featuring bulky polychlorinated cations,[131−133] consistently reveals Re−Re distances in the range 2.70−2.725 Å.

For this complex, VWN is the only DFT approach among those surveyed here to show good agreement with the experimental bond length (see Figure 1), with all other methods substantially exceeding the target bond length range. As a third-transition-row complex, however, we would expect that relativistic effects are important for this complex, and the exclusion of correction terms for such effects would likely lead to overestimation of the Re−Re bond length. The influence of relativistic effects in calculations on this species is explicitly explored in subsection 1.9 below.

1.8. $Rh_2(O_2CCH_3)_4(CO)_2$. This complex, one of a large number of axially ligated dirhodium tetraacetate structures, has been crystallographically characterized[134] to have a Rh−Rh bond length of 2.42 Å, a value typical of this class of compounds.[1] No previous DFT or other structural calculations on this species appear to have been reported. The performance of the various methods surveyed here, for this species, is remarkable in the sense that all nine methods deliver optimized Rh−Rh separations within a mere 0.05 Å range which lies tantalizingly close to, but does not overlap, the defined target range of 2.42 ± 0.05 Å. Among the other neutral or singly charged complexes surveyed here, only $Mo_2(NH_2)_6$ yields such a compact range of bond lengths (but in that case all methods achieve the target accuracy, whereas no method is entirely satisfactory for the rhodium complex). Given the consistent overestimation by all methods, it is hardly surprising that in this one instance the most overbinding technique, VWN, delivers the best Rh−Rh bond length while B-LYP, shown by several previous examples to be prone to bond length exaggeration, again produces the largest result.

1.9. Relativistic Effects. We have used the ZORA (zeroth-order regular approximation) formalism[73,74] to study the influence of including relativistic corrections in geometry optimizations on the species $Mo_2(H_2PCH_2PH_2)_2Cl_6$, $Mo_2(NH_2)_6$, and $Re_2Cl_9^-$, using the nine DFT approaches surveyed here, with results summarized in Table 2. It is clear that, in accordance with general expectations regarding relativistic effects, the impact of the ZORA corrections is greatest on the third-transition-row-atom-containing complex $Re_2Cl_9^-$, with Re−Re bond contractions of 0.21−0.44 Å. The edge-shared molybdenum dimer $Mo_2(H_2PCH_2PH_2)_2Cl_6$ is rather less sensitive to relativistic correction, with B-LYP exhibiting the most extreme Mo−Mo bond contraction of 0.07 Å for this species, in contrast to the mild (∼0.01 Å) Mo−Mo bond elongations shown by several DFT methods for this complex. Finally, the unsupported Mo−Mo bond of the $Mo_2(NH_2)_6$ complex is consistently lengthened by a small

(123) Filatov, M.; Thiel, W. *Mol. Phys.* **1997**, *91*, 847.
(124) Tsuneda, T.; Suzumura, T.; Hirao, K. *J. Chem. Phys.* **1999**, *110*, 10664.
(125) Liu, X. Y.; Alvarez, S. *Inorg. Chem.* **1997**, *36*, 1055.
(126) Ziegler, T. *J. Am. Chem. Soc.* **1983**, *105*, 7543.
(127) Bursten, B. E.; Cotton, F. A.; Green, J. C.; Seddon, E. A.; Stanley, G. G. *J. Am. Chem. Soc.* **1980**, *102*, 4579.
(128) Chisholm, M. H.; Cotton, F. A.; Frenz, B. A.; Reichert, W. W.; Shive, L. W.; Stults, B. R. *J. Am. Chem. Soc.* **1976**, *98*, 4469.
(129) Bonati, F.; Cotton, F. A. *Inorg. Chem.* **1967**, *6*, 1353.
(130) Heath, G. A.; McGrady, J. E.; Raptis, R. G.; Willis, A. C. *Inorg. Chem.* **1996**, *35*, 6838.
(131) Hauck, H. G.; Klingelhofer, P.; Muller, U.; Dehnicke, K. *Z. Anorg. Allg. Chem.* **1984**, *510*, 180.
(132) Baranov, A. I.; Khyvorykh, G. V.; Troyanov, S. I. *Z. Anorg. Allg. Chem.* **1999**, *625*, 1240.
(133) Rabe, S.; Muller, U. *Z. Anorg. Allg. Chem.* **2000**, *626*, 830.
(134) Christoph, G. G.; Koh, Y. B. *J. Am. Chem. Soc.* **1979**, *101*, 1422.

Table 2. Influence of ZORA Scalar Relativistic Corrections on Optimized Metal−Metal Distances for $Mo_2(H_2PCH_2PH_2)_2Cl_6$, $Mo_2(NH_2)_6$, and $Re_2Cl_9^-$

	$Mo_2(H_2PCH_2PH_2)_2Cl_6$ 2.73−2.83 Å[a]		$Mo_2(NH_2)_6$ 2.21 Å[a]		$Re_2Cl_9^-$ 2.70−2.73 Å[a]	
method	r_e(Mo−Mo)[b]	Δr_e(ZORA)[c]	r_e(Mo−Mo)[b]	Δr_e(ZORA)[c]	r_e(Re−Re)[b]	Δr_e(ZORA)[c]
VWN	2.680	0	*2.202*	0	2.413	−0.31
VWN+B-LYP	*2.750*	+0.01	*2.234*	+0.01	2.451	−0.42
PW91	*2.831*	+0.01	*2.241*	+0.01	*2.722*	−0.23
PBE	*2.830*	+0.01	*2.244*	+0.02	*2.724*	−0.23
BP	2.850	−0.01	*2.244*	+0.01	*2.746*	−0.27
Xα	*2.809*	+0.01	*2.243*	+0.01	*2.683*	−0.21
revPBE	2.853	−0.03	*2.247*	+0.01	2.897	−0.39
RPBE	2.859	−0.05	*2.249*	+0.01	2.920	−0.40
B-LYP	2.878	−0.07	2.267	+0.01	2.957	−0.44

[a] M−M distance range embodied in previously reported crystallographic studies, as identified within the text for each complex. [b] Optimized, ZORA-corrected, metal−metal separation in angstroms according to the indicated DFT method. All calculations were performed using the broken-symmetry technique of Noodleman and Norman (ref 67). [c] Change in optimized metal−metal separation, in angstroms, resulting from inclusion of the ZORA scalar relativistic correction.

increment when ZORA is incorporated, regardless of the DFT method used. These disparate results for the three different complexes suggest that relativistic corrections are indeed apparently necessary to achieve good optimized geometries for gradient-corrected DFT calculations on dinuclear complexes containing third-transition-row metal atoms: the PW91 and PBE methods, in particular, perform extremely well for $Re_2Cl_9^-$ when ZORA corrections are implemented, but all of the orthodox gradient-corrected methods show considerable improvement with ZORA for this species. In contrast, the superior performance of VWN and VWN+B-LYP in uncorrected optimizations is seen to be largely fortuitous and may be ascribed to the compensation by "overbinding" for the lack of relativistic Re−Re bond stabilization. ZORA inclusion appears much less important for second-row (and, we expect, first-row) transition metal complexes than for third-row species: although, in most instances, for edge-shared $Mo_2(H_2PCH_2PH_2)_2Cl_6$ the influence of relativity is to change the Mo−Mo distance in the right direction, the magnitude of this change is insufficient in any case to move the calculated bond length into the "target range", and this is largely the experience also for $Mo_2(NH_2)_6$ where the ZORA-induced bond length change often appears to be slightly counterproductive.

1.10. General Appraisal of Method Performance. While the calculated M−M separations listed in Table 1 cannot serve to fully establish or undermine the reliability of any of the DFT methods tested here, they nevertheless allow some reasonably strong recommendations on the usage of various functionals. On the basis of our experience in the present work, we caution against the use of the VWN local density functional in isolation, and of the B-LYP, RPBE, and revPBE gradient-corrected functionals, in calculations on neutral or singly charged dinuclear complexes. The VWN functional is prone to bond length underestimation by a substantial margin, implying that it exhibits an unwarranted preference for strongly metal−metal bonded configurations of such complexes, while B-LYP, RPBE, and (to a lesser extent) revPBE suffer from the reverse defect, in the sense that they often lead to optimized geometries in which the direct metal−metal interaction is underemphasized. It is worth noting that the countervailing shortcomings of VWN and B-LYP can to a large extent be neutralized when these methodologies are combined in the VWN+B-LYP approach explored here, but since this "unorthodox" approach does not outperform other standard approaches for mildly charged dinuclear complexes we cannot recommend VWN+B-LYP in this regard either. The best performance across the Table 1 "test set" is exhibited by PW91, for which all our optimized metal−metal bond lengths are within ±0.1 Å of the range of experimentally observed results, but the performance of PBE is very similar to PW91, and BP is not significantly inferior. It is intriguing to note that the Xα method, which many practitioners would now consider an outmoded approach, actually performs quite well in competition with the latter three gradient-corrected functionals, but it is nevertheless probable that PW91, PBE, and BP are generally viewed as the preferred methods on the basis of our survey.

2. Multiply Charged Dinuclear Complexes. Results of geometry optimizations for the complexes within this category are presented in Table 3, which uses the same definition of the "target range", and the same ordering of DFT methods, as featured in Table 1.

2.1. $Cr_2(CH_3)_8^{4-}$. This Cr(II)-containing tetraanion has been characterized within crystalline $Li_4Cr_2(CH_3)_8{\cdot}4C_4H_8O$.[135] The crystallographic Cr−Cr distance is 1.980 Å. Synthesis of related compounds $Li_4Cr_2(CH_2R)_8{\cdot}4C_4H_8O$ (R = C_6H_5, $(CH_3)_3C$, $(CH_3)_2C(C_6H_5)$) has also been reported, with these more sterically cluttered species displaying greater lability.[136] Experimental studies of the spectroscopy[137] and reactivity[136,138] of $Cr_2(CH_3)_8^{4-}$ have also been undertaken, and it is interesting to note that reversible cleavage of the (nominally quadruple) Cr−Cr bond has been reported.[138] Several previous theoretical studies also exist, which have used INDO,[139] SCF,[99,140] APSG (antisymmetric product of strongly orthogonal geminals),[140] and configuration interaction.[99] The last of these methods, which represents also the highest level of

(135) Krausse, J.; Marx, G.; Schoedl, G. *J. Organomet. Chem.* **1970**, *21*, 159.
(136) Hao, S.; Song, J.-I.; Berno, P.; Gambarotta, S. *Organometallics* **1994**, *13*, 1326.
(137) Sattelberger, A. P.; Fackler, J. P. *J. Am. Chem. Soc.* **1977**, *99*, 1258.
(138) Hao, S.; Gambarotta, S.; Bensimon, C. *J. Am. Chem. Soc.* **1992**, *114*, 3556.
(139) Correa de Mello, P.; Edwards, W. D.; Zerner, M. C. *Int. J. Quantum Chem.* **1983**, *23*, 425.
(140) Guest, M. F.; Hillier, I. H.; Garner, C. D. *Chem. Phys. Lett.* **1977**, *48*, 587.

Table 3. Optimized Metal−Metal Distances Obtained for Multiply Charged Dinuclear Complexes

		r(M−M)[b]/Å									
species	structural motif[a]	expt[c]	VWN	VB[d]	PW91	PBE	BP	Xα	revPBE	RPBE	B-LYP
$Cr_2(CH_3)_8^{4-}$ [e]	NB	1.98	1.817	1.901	–	–	–	–	–	–	–
$Mo_2(NCCH_3)_8^{4+}$	NB	2.19	2.178	2.194	2.232	2.223	2.239	2.229	2.236	2.240	2.257
$Mo_2Cl_8^{4-}$	NB	2.13−2.14	*2.160*	*2.184*	2.232	2.234	2.242	2.239	2.249	2.256	2.259
$Mo_2Cl_9^{3-}$	FS	2.52−2.82	2.379	2.408	3.053	3.060	3.280	2.987	3.362	3.390	3.445
$Mo_2I_9^{3-}$	FS	3.07	2.968	*3.049*	3.637	3.773	3.681	3.582	3.880	3.885	3.924
$W_2Cl_9^{3-}$	FS	2.42−2.50	*2.442*	*2.485*	2.864	2.884	2.911	2.667	2.987	3.022	2.927
$Ru_2(NH_2)_2(NH_3)_8^{4+}$	ES	2.63	*2.672*	2.735	2.754	2.774	2.769	2.726	2.789	2.793	2.775
$Rh_2(NCCH_3)_8(NCH)_2^{4+}$	NB	2.62	2.712	2.843	2.851	2.874	2.860	2.789	2.955	2.965	2.927

[a] ES = edge-shared bioctahedral complex; FS = face-shared bioctahedral complex; PW = paddlewheel (tetracarboxylate) complex; NB = nonbridged complex. [b] Optimized metal−metal separation according to the indicated method. All calculations were performed with TZP basis sets, using the broken-symmetry technique of Noodleman and Norman (ref 67). [c] M−M distance range embodied in previously reported crystallographic studies, as identified within the text for each complex. [d] VB = VWN+B-LYP (see text for details). [e] In many instances (shown by a dash in the appropriate column), this complex was not stable against dissociation to $2Cr(CH_3)_4^{2-}$ for a given DFT technique.

theory used in the studies to date, indicates a Cr−Cr bond length of 2.16 Å, in fair agreement with experiment.

The results of our own calculations (see Table 3; see also Figure 2) are illuminating. Only the "overbinding" VWN and VWN+B-LYP methods succeed in delivering a broken-symmetry local minimum, although both approaches significantly underestimate the bond length; all other methods result in fragmentation of the (formally quadruple) Cr−Cr bond. The failure of all the "orthodox" gradient-corrected methods may well indicate that the gas-phase $Cr_2(CH_3)_8^{4-}$ anion does indeed spontaneously fragment, due to coulombic factors. Nevertheless, the inability of the gradient-corrected methods to deliver results capable of affording insight into the bonding within a crystallographically known multiply charged complex stands in contrast to the reasonable success shown by the notionally "inferior" methods VWN and VWN+B-LYP for this species. This counterintuitive result brings us back to the often-raised comment that "the overbinding tendencies of VWN" (and by extension, similar correlation-dominated methods) are serendipitously advantageous in treating multiply charged dinuclear complexes, perhaps due to a fortuitous cancellation of errors.

2.2. $Mo_2(NCCH_3)_8^{4+}$. This species has been synthesized in association with the $F_3CSO_3^-$ and BF_4^- counterions,[141,142] with the crystal structure for the latter system[142] yielding the sole experimental bond length determination of 2.187 Å. All of the DFT methods surveyed performed well for this species, with only B-LYP giving a result in (marginal) excess of the target range. In contrast to $Cr_2(CH_3)_8^{4-}$ (see above), which shares the same absolute charge, metal atom oxidation state, valence d electron count, and formal metal−metal bond order, this quadruple bond is evidently sufficiently robust that it can withstand coulombic explosion outside of the stabilizing crystalline environment.

2.3. $Mo_2Cl_8^{4-}$. In keeping with the previous two examples, this quadruply charged complex is another d^4d^4 quadruply metal−metal bonded species. Salts containing the potassium, ethylenediammonium, and diprotonated piperazine countercations[143−145] have been characterized by X-ray crystallography, yielding Mo−Mo separations ranging from 2.129 to 2.139 Å, while resonance Raman and electronic spectra of several of these systems, and of the analogous cesium, rubidium, and ammonium salts, have also been reported.[146] The narrow range in experimental bond lengths, and comparison with the structurally related $Mo_2(NCCH_3)_8^{4+}$ complex (see above), identify this as another strongly bonded species. Accordingly, all DFT methods again deliver optimized Mo−Mo distances in fair to good agreement with experiment (see Figure 2), although it is notable that all of the orthodox gradient-corrected approaches assign a longer bond to this species than to $Mo_2(NCCH_3)_8^{4+}$ in a reversal of the trend seen experimentally. None of the methods tested undercuts the experimental result, and only VWN and VWN+B-LYP are formally within the target range.

2.4. $Mo_2Cl_9^{3-}$. This nonahalide trianion has been characterized as a subunit within a wide variety of salts, with general forms including $A^I_3Mo_2Cl_9$, $A^{II}BMo_2Cl_9$, and $A^{II}_{1.5}Mo_2Cl_9$.[20−24,26−31,147] The wide variation in Mo−Mo bond distances, from 2.52 to 2.82 Å,[24,28,31] contrasts notably with the apparent rigidity of several other face-shared nonahalide dimers, such as $W_2Cl_9^{3-}$ (see below); in a recent survey of crystallographic results, $Mo_2Cl_9^{3-}$ stands out as a complex having a particularly deformable metal−metal bond.[148]

Aside from our own earlier theoretical investigations,[3−6] $Mo_2Cl_9^{3-}$ has previously been subjected to study using the Xα standing wave approach[149] and the CASSCF technique:[49] however, neither of the latter studies featured any mode of geometry optimization.

In contrast to the two immediately preceding molybdenum complexes, $Mo_2Cl_9^{3-}$ is a species for which the problems associated with gas-phase calculation on a multiply charged species are compounded by the extreme plasticity of the metal−metal bond, and these two degrees of difficulty are reflected in the overall very poor performance of the various DFT approaches for this species. VWN and VWN+B-LYP give Mo−Mo distances which correspond approximately to those expected for a full triple Mo−Mo bond, while at the

(141) Mayer, J. M.; Abbott, E. H. *Inorg. Chem.* **1983**, *22*, 2774.
(142) Cotton, F. A.; Wiesinger, K. J. *Inorg. Chem.* **1991**, *30*, 871.
(143) Brencic, J. V.; Cotton, F. A. *Inorg. Chem.* **1969**, *8*, 7.
(144) Brencic, J. V.; Cotton, F. A. *Inorg. Chem.* **1969**, *8*, 2698.
(145) Leban, I.; Segedin, P. *Inorg. Chim. Acta* **1984**, *85*, 181.
(146) Clark, R. J. H.; Franks, M. L. *J. Am. Chem. Soc.* **1975**, *97*, 2691.
(147) Smith, P. W. University College: London, 1962.
(148) Orpen, A. G.; Quayle, M. J. *J. Chem. Soc., Dalton Trans.* **2001**, 1601.
(149) Ginsberg, A. P. *J. Am. Chem. Soc.* **1980**, *102*, 111.

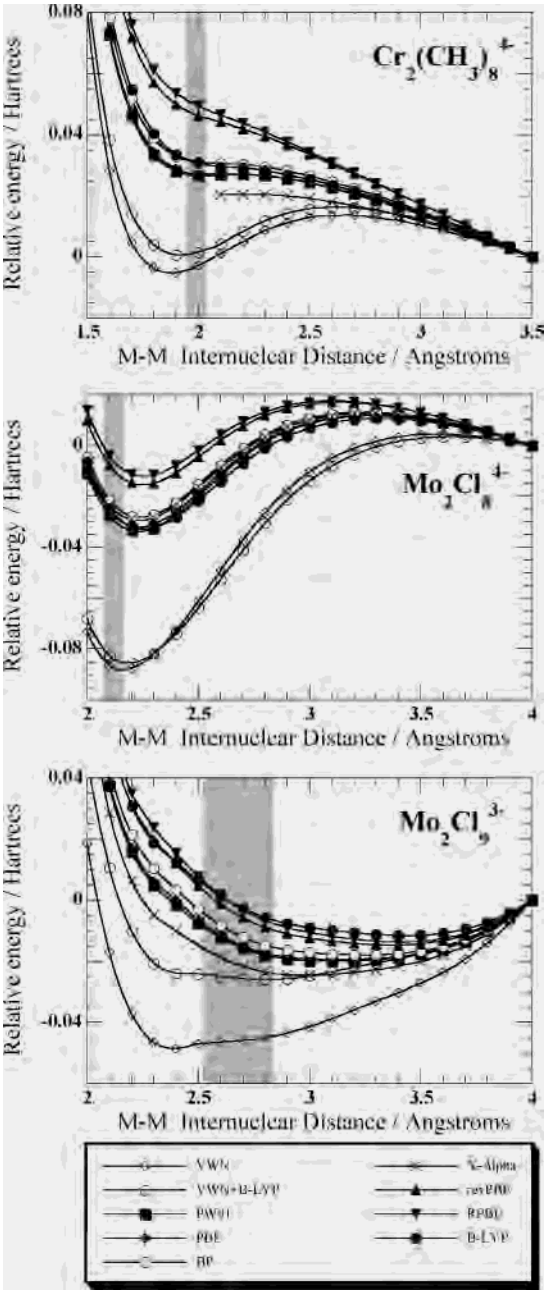

Figure 2. Potential energy curves, obtained using the broken-symmetry (BS) technique and the indicated density functional methodology, for the dinuclear complexes $Mo_2Cl_9^{3-}$, $Mo_2I_9^{3-}$, $Re_2Cl_9^{-}$, $W_2Cl_9^{3-}$, and $V_2Cl_3(OMe_2)_6^{+}$. Energy values for all functionals are expressed relative to the total energy of the partially optimized structure at the largest modeled M−M separation, while the "target range" encompassing the experimentally observed range of M−M distances (as defined in the text) is shown in gray.

other extreme B-LYP and RPBE exceed the VWN value by more than 1 Å. Of the orthodox gradient-corrected approaches, PBE and PW91 perform best, but their values are still more than 0.2 Å above the upper edge of the broad target range; they are arguably outshone here by VWN+B-LYP which is 0.12 Å too short to reach the target range. The difficulty of all methods in reproducing the experimental geometry is highlighted in Figure 2.[150]

The extreme variability in the experimental Mo−Mo distance, as a function of the crystalline environment, has been attributed to the coplanar location of the univalent countercations and the bridging chloride anions in crystals of the formula $A^{I}_3Mo_2Cl_9$. A direct relation has been reported[30,31] between the steric demands of the cation and the Mo−Mo bond elongation: the larger the cation, the greater the compression of the (μ-Cl)$_3$ bridge unit and hence the greater the resultant Mo−Mo separation.[30] This counterion-induced structural distortion, which undoubtedly is abetted by the comparative shallowness of the potential energy well surrounding the minimum-energy structure, is not modeled by the vacuum-phase geometry optimizations which we have performed on $Mo_2Cl_9^{3-}$. It is well worth noting, also, that when the structural formula includes divalent countercations, as in the examples $(bipyH_2)^{II}(HOCH_2CH_2NH_3)^{I}Mo_2Cl_9$,[29] $(4\text{-}NH_3pyH)^{II}(HOCH_2CH_2NH_3)^{I}Mo_2Cl_9$,[29] and $(enH_2)_2{}^{II}Mo_2Cl_9\cdot Cl$,[26] the countercations are not confined to the bridging plane, and in this circumstance, the range of Mo−Mo distances seen is much narrower, viz., 2.585−2.619 Å.[27,29] If we assess the various functionals against this tighter range, none of the functionals used in vacuum-phase calculations deliver a "correct" bond length and only VWN+B-LYP returns a distance within 0.2 Å. Thus, even if the counterion-induced structural distortion of the $Mo_2Cl_9^{3-}$ framework is effectively removed from consideration, $Mo_2Cl_9^{3-}$ remains a particularly challenging structure to satisfactorily characterize.

Finally, we note that while the present survey is formally limited to assessment of "pure" density functionals, the performance of 'hybrid' density functional methods such as B3-LYP in the context of metal−metal bonding is also of interest. We have performed broken-symmetry B-LYP/SDD and B3-LYP/SDD optimizations of $Mo_2Cl_9^{3-}$, using the GAUSSIAN98 program suite;[83] these calculations return optimized Mo−Mo distances of 3.557 and 3.567 Å, respectively. The difference between the B-LYP/TZP (from ADF2002) and B-LYP/SDD (from GAUSSIAN98) optimized bond lengths shows, unsurprisingly, that the $Mo_2Cl_9^{3-}$ structure is as sensitive to choice of basis sets as to other factors including the chosen density functional.[151] It is worth noting here that B3-LYP also fared no better than B-LYP in the calculations reported by Andersson et al.[48] on $Cr_2(O_2CCH_3)_4$ (see above), which like $Mo_2Cl_9^{3-}$ is a dinuclear complex for which a particularly broad range of intermetallic separations has been reported from laboratory studies. The

(150) As with $V_2Cl_3(O(CH_3)_2)_6^{+}$ [94] and $Mo_2(H_2PCH_2PH_2)_2Cl_6$,[122] we have attempted an assessment of meta-GGA performance for $Mo_2Cl_9^{3-}$. In this instance, to compensate for the structural sensitivity to coulombic effects, we performed linear transits using VWN+B-LYP, PBE, and B-LYP representing methods identified from our neutral and singly charged complex calculations as, respectively, overbinding, approximately "correct", and underbinding. In the resulting meta-GGA single-point calculations, only the FT97 method[123] performed well, with Mo−Mo ∼ 2.95 Å when VWN+B-LYP was used to provide the geometries, and the xc potential, for the meta-GGA "scan", and Mo−Mo ∼ 2.85 Å when either PBE or B-LYP was used as the underlying DFT method for which the meta-GGA energies were evaluated. For this species, all methods using the KCIS correlation functional[96] collapsed as the Mo−Mo distance was decreased, while other meta-GGAs assessed consistently overestimated Mo−Mo with values of 3.4 Å or larger. The inconsistency seen with the various meta-GGAs for the three compounds assessed[94,122] indicates, at least, that none of these methods can be seen as an especially promising substitute for the DFT methods for which broken-symmetry calculations are currently feasible.

admittedly limited data at hand therefore suggests that B3-LYP, generally regarded as one of the most reliable extant hybrid density functionals, does not perform particularly well in the context of characterizing metal−metal bond lengths (except in the strongly multiply bonded limit, for which it has been shown to be quite successful).[50,51]

2.5. $Mo_2I_9^{3-}$. Synthesis of this complex has been reported in conjunction with the Cs^+ and $CH_3CH_2NH_3^+$ counterions,[25,30,31] although only the former combination has been characterized through crystallography.[30] The recorded Mo−Mo bond distance of 3.07 Å suggests a smaller degree of metal−metal bonding than is seen in $Mo_2Cl_9^{3-}$. Our calculated Mo−Mo bond lengths for $Mo_2I_9^{3-}$ (see Table 3) support this suggestion, with all methods yielding Mo−Mo distances at least 0.4 Å larger than the corresponding $Mo_2Cl_9^{3-}$ value; however, the absolute performance is little better than that seen for $Mo_2Cl_9^{3-}$. All of the orthodox gradient-corrected methods, and Xα, overestimate the metal−metal distance very considerably, while VWN again undercuts the experimental result. Only VWN+B-LYP strikes the appropriate balance (between overbinding and coulombic distortion?) with a calculated distance within 0.03 Å of the crystallographic value.

2.6. $W_2Cl_9^{3-}$. This face-shared dimer was first identified as a discrete structural unit in solution;[32] powder diffraction studies[33] subsequently revealed the dimeric structure, for which a W−W bond order of two was ascribed by Pauling.[152] There is considerable additional evidence of a strong metal−metal bond in this species.[8,13,34,36−43] The W−W distance shows comparatively little variation (2.41, 2.42, and 2.50 Å, respectively) in the three crystalline compounds $K_3W_2Cl_9$,[35] $(HTMPP)_3W_2Cl_9$,[44] and $Cs_3W_2Cl_9$, further indicating a highly rigid structure for this trianion.

The DFT performance seen for this species broadly matches that evident in the other multiply charged face-shared complexes noted above: none of the gradient-corrected methods gives a bond length short enough to fit within the target range, while the overbinding propensity of VWN and of VWN+B-LYP appears to compensate quite well for the coulombic stress suffered by the vacuum-phase structure.

2.7. $Ru_2(NH_2)_2(NH_3)_8^{4+}$. This edge-shared d^5d^5 complex, isolated with chloride counterions, has been characterized by crystallography.[153] The experimental bond length is exceeded by all nine DFT approaches tested here, although VWN gives a result close enough to occupy the target range, and at less than 0.13 Å, the spread of values from shortest to longest is considerably more compressed than is found for any of the face-shared complexes. As has been seen for many of the other complexes surveyed here, VWN+B-LYP yields a value lower than any of the orthodox gradient-corrected methods, with B-LYP and RPBE among the most excessive approaches.

2.8. $Rh_2(NCCH_3)_8(NCH)_2^{4+}$. This species is a close congener to $Rh_2(NCCH_3)_{10}^{4+}$, which has been subjected to crystallographic characterization in several forms.[154−156] The substitution of the two terminal acetonitrile ligands by HCN in our calculations was undertaken so as to permit calculation in C_{4v} symmetry, at substantially reduced computational cost, in contrast to the requirement for C_s symmetry imposed by retaining terminal CH_3CN. It is likely that coulombic distortion, rather than our virtual ligand-switching, is responsible for the systematic overestimation of the Rh−Rh bond length in our calculations, although it is also worth commenting that the two rhodium-containing complexes studied in the present work (one neutral, one quadruply charged) are the only two species for which all DFT methods, including VWN and VWN+B-LYP, yield results which lie above the upper limit of the target range. This may indicate a problem with the rhodium basis set employed here, although further study seems required to substantiate this suggestion.

2.9. Relativistic Effects. We have assessed the influence of ZORA scalar relativistic corrections[73,74] on geometry optimization for our sole multiply charged third-transition-row dinuclear complex $W_2Cl_9^{3-}$, as well as for the comparatively challenging second-row examples $Mo_2Cl_8^{4-}$ and $Mo_2Cl_9^{3-}$. The results (see Table 4) largely parallel the outcome of the ZORA analysis described, for the neutral and singly charged complexes, in subsection 1.9. By far the largest impact seen here is for $W_2Cl_9^{3-}$, for which all six orthodox gradient-corrected methods yield W−W bond contractions of 0.35 Å or greater. In most instances this compression of the W−W axis is sufficient to achieve the target accuracy: even B-LYP, frequently maligned elsewhere in the present work, shows a dramatic improvement from 2.927 Å (uncorrected) to 2.458 Å (with ZORA). Bond length changes for the "local density" methods Xα and VWN, and for unorthodox VWN+B-LYP, are notably less dramatic, but for these methods the optimized W−W distance without ZORA correction is considerably closer to the strongly bonded limit than is the case for the orthodox gradient-corrected methods (see Table 3), implying a more limited scope for bond truncation.

The analogous $Mo_2Cl_9^{3-}$ complex, which we[5,30] and other researchers[148] have singled out as an extraordinarily flexible molecular structure, is distinctly less subject to relativistic influence than its tungsten-containing counterpart. Only for BP do we see a decrease in the Mo−Mo distance of greater

(151) We have not pursued B3-LYP, or other hybrid density functional, optimizations on any of the other dinuclear complexes in the present study, for reasons of computational expediency. The ADF2002 program suite does not include hybrid functionals amongst its repertoire, while broken-symmetry calculations on $Mo_2Cl_9^{3-}$ using GAUSSIAN98, with even a modest metal and ligand basis set, are extremely CPU-time-consuming. Since almost all of the other dinuclear complexes in our test set are more structurally complex than $Mo_2Cl_9^{3-}$, it was judged that attempting B3-LYP optimizations in broken symmetry for such species would be prohibitively computationally expensive.

(152) Pauling, L. *The Nature of the Chemical Bond*, 3rd ed.; Cornell University Press: Ithaca, NY, 1960.
(153) Flood, M. T.; Ziolo, R. F.; Earley, J. E.; Gray, H. B. *Inorg. Chem.* **1973**, *12*, 2153.
(154) Baranovskii, I. B.; Golubnichaya, M. A.; Zhilyaev, A. N.; Shchelokov, R. N. *Zh. Neorg. Khim.* **1984**, *29*, 1520.
(155) Baranovskii, I. B.; Zhilyaev, A. N.; Dikareva, L. M. *Zh. Neorg. Khim.* **1988**, *33*, 3123.
(156) Dunbar, K. R. *J. Am. Chem. Soc.* **1988**, *110*, 8247.

Table 4. Influence of ZORA Scalar Relativistic Corrections on Optimized Metal−Metal Distances for $Mo_2Cl_8^{4-}$, $Mo_2Cl_9^{3-}$, and $W_2Cl_9^{3-}$

	$Mo_2Cl_8^{4-}$ 2.13−2.14 Å[a]		$Mo_2Cl_9^{3-}$ 2.52−2.82 Å[a]		$W_2Cl_9^{3-}$ 2.42−2.50 Å[a]	
method	r_e(Mo−Mo)[b]	Δr_e(ZORA)[c]	r_e(Mo−Mo)[b]	Δr_e(ZORA)[c]	r_e(W−W)[b]	Δr_e(ZORA)[c]
VWN	*2.181*	+0.02	2.370	−0.01	2.400	−0.04
VWN+B-LYP	2.217	+0.03	2.407	0	*2.423*	−0.06
PW91	2.270	+0.04	3.031	−0.02	*2.428*	−0.44
PBE	2.269	+0.04	2.964	−0.10	*2.430*	−0.43
BP	2.267	+0.03	3.092	−0.19	*2.417*	−0.49
Xα	2.260	+0.02	3.006	+0.02	*2.426*	−0.24
revPBE	2.284	+0.04	3.270	−0.09	*2.438*	−0.55
RPBE	2.288	+0.03	3.330	−0.06	2.668	−0.35
B-LYP	2.285	+0.03	3.377	−0.07	*2.458*	−0.47

[a] M−M distance range embodied in previously reported crystallographic studies, as identified within the text for each complex. [b] Optimized, ZORA-corrected, metal−metal separation in angstroms according to the indicated DFT method. All calculations were performed using the broken-symmetry technique of Noodleman and Norman (ref 67). [c] Change in optimized metal−metal separation, in angstroms, resulting from inclusion of the ZORA scalar relativistic correction.

than 0.1 Å, although in almost all instances the ZORA-corrected values represent a modest improvement over the uncorrected geometries. Nevertheless, ZORA-corrected or not, none of the tested functionals delivers an optimized geometry which falls within the broad experimental range 2.52−2.82 Å.

The Mo^{II} complex, $Mo_2Cl_8^{4-}$, features an unsupported metal−metal bond. As seen also in subsection 1.9 for the nonbridged example $Mo_2(NH_2)_6$, inclusion of relativistic effects induces a slight elongation of the Mo−Mo bond for all DFT methods, leading to a correspondingly greater divergence from the experimental Mo−Mo distance than is obtained upon calculation without relativistic corrections.

2.10. Frequency Calculations. There are obvious limitations to the applicability of the calculated metal−metal separation as a yardstick for the performance of the various DFT methods surveyed. In many respects, comparison of the calculated vibrational frequencies for different complexes, as obtained from various DFT treatments, would permit a more detailed analysis than we have undertaken here. Unfortunately, two principal problems obstruct such an assessment of DFT reliability by way of vibrational frequency calculation. First, many of the dinuclear complexes which have been crystallographically characterized have not been subjected to in-depth spectroscopic studies, particularly the Raman spectroscopic investigations which are required to detect the vibrational modes associated with metal−metal stretching in symmetric complexes.[157−159] Second, the calculation of vibrational frequencies for complexes featuring polyatomic ligands is feasible only using quantum chemical program suites which employ analytic second derivatives; computation of frequencies via numerical double-differentiation, which is the technique currently implemented in ADF2002,[70] is much more demanding of computational resources. With these two considerations in mind, we have been able to identify only $Mo_2Cl_8^{4-}$,[146,160] $Mo_2Cl_9^{3-}$,[25,161] and $W_2Cl_9^{3-}$ [13] among the complexes surveyed here as being species for which vibrational frequency calculation is worthwhile. We have also calculated vibrational frequencies for the related face-shared complex $Cr_2Cl_9^{3-}$,[13,161] which ostensibly lacks a direct metal−metal bond: this is not one of the dimers considered in the earlier sections of this survey, but it merits vibrational analysis as a rare example of a dinuclear complex for which polarized Raman spectroscopy data are available.[162] Note that, as is the case with the M−M bond length analysis presented above, it is the ability of the DFT method to replicate condensed-phase vibrational properties of the complexes, and not the precision with which the DFT method returns (in any event unknown) gas-phase vibrational parameters, which is the criterion we use here to evaluate the performance of the various density functional approaches.

Our calculated vibrational spectra are summarized in Table 5. For Mo_2Cl_8,$^{4-}$ the Mo−Mo stretching transition is unambiguously assigned, both from the spectroscopic data[146,160] and from our calculations. As with the trend evident in calculated M−M bond lengths seen in Table 3, VWN and VWN+B-LYP deliver the ν(Mo−Mo) values closest to that observed experimentally; B-LYP and RPBE equally fare worst, with the most severe underestimation of ν(Mo−Mo) for this complex. The unbridged octachloride complex is, however, the only species in Table 5 possessing a unique M−M stretching mode. For all of the face-shared $M_2Cl_9^{3-}$ complexes, the (calculated and observed) spectra exhibit several modes in which "breathing" motion of the bridging Cl_3 unit is inferred to occur in conjunction with M−M stretching. Comparison of our calculated spectra for $Cr_2Cl_9^{3-}$, with the polarized Raman data of Black et al.,[162] indicates that the 2 A_1' and 4 A_1' modes are associated with the greatest degree of axial motion of the two Cr atoms: frequencies for both of these modes are consistently underestimated by all of the DFT methods surveyed, although VWN delivers conspicuously the closest, and B-LYP the least satisfactory, match for 4 A_1'. We have also included in Table 5 the calculated values for the intense, highest-frequency E' symmetry (doubly degenerate) mode which is a distinctive

(157) Ketteringham, A. P.; Oldham, C. *J. Chem. Soc., Dalton Trans.* **1973**, 1067.
(158) Clark, R. J. H. *J. Mol. Struct.* **1980**, *59*, 137.
(159) Shriver, D. F.; Cooper, C. B., III. *Adv. Infrared Raman Spectrosc.* **1980**, *6*, 127.
(160) Angell, C. L.; Cotton, F. A.; Frenz, B. A.; Webb, T. R. *J. Chem. Soc., Chem. Commun.* **1973**, 399.
(161) Grey, I. E.; Smith, P. W. *Aust. J. Chem.* **1969**, *22*, 1627.
(162) Black, J. D.; Dunmuir, J. T. R.; Forrest, I. W.; Lane, A. P. *Inorg. Chem.* **1975**, *14*, 1257.

Table 5. Comparison of Key Calculated Vibrational Frequencies (in cm^{-1}) with Spectroscopic Literature Values, for the Dinuclear Complexes $Mo_2Cl_8^{4-}$ and $M_2Cl_9^{3-}$ (M = Cr, Mo, W)

	$Mo_2Cl_8^{4-}$	$Cr_2Cl_9^{3-}$			$Mo_2Cl_9^{3-}$	$W_2Cl_9^{3-}$		
method	ν(M−M)[a] 338−348[a,b]	ν(2 A_1')[c] 200−206[b,c]	ν(4 A_1')[c] 378−393[b,c]	$\nu(I_{vs}(E'))$[d] 315−342[b,d]	$\nu(I_{vs}(E'))$[e] 320−342[b,e]	$\nu(I_{vs}(E'))$[f] 311−313[b,f]	MD[g]	MAD[h]
VWN	381	173	330	296	338	306	−4.6	9.0
VWN+B-LYP	323	178	303	265	297	277	−13.4	13.4
PW91	314	176	305	268	282	270	−14.9	14.9
PBE	311	175	302	266	283	262	−15.7	15.7
BP	307	175	300	262	273	264	−16.6	16.6
Xα	304	170	311	276	295	278	−14.1	14.1
revPBE	301	173	289	251	263	250	−19.3	19.3
RPBE	296	172	286	247	259	247	−20.4	20.4
B-LYP	296	172	283	246	255	250	−20.6	20.6

[a] Metal−metal stretching frequency as identified in ref 146. [b] Experimentally observed range of frequencies, from the indicated reference. [c] A_1' symmetry vibrational modes displaying a major component due to metal−metal stretching (according to our calculations). The second and fourth A_1' modes (D_{3h} symmetry assigned overall) detailed in a polarized Raman study (ref 162) correspond, in our C_{3v} broken-symmetry calculations, to the third and seventh A_1-symmetry modes, respectively. [d] Frequency of the "very strong" E'-symmetry mode reported in ref 13. [e] Frequency of the "very strong" E'-symmetry mode reported in ref 25. [f] The "very strong" high-frequency mode reported for several $W_2Cl_9^{3-}$ compounds (ref 13). Note that, as discussed in the text, we assign this to an E′-symmetry mode rather than due to the A_2''-symmetry transition identified in ref 13. [g] Mean deviation for the method indicated, expressed as a percentage of the median experimentally observed frequency. [h] Mean absolute deviation for the method indicated, expressed as a percentage of the median experimentally observed frequency.

feature within the experimental infrared spectrum:[13] again, all DFT methods fall short, with the performance trends matching that noted for 4 A_1'. In the absence of a clear assignment of the most significant M−M stretching mode (s) in laboratory spectra of $Mo_2Cl_9^{3-}$ and $W_2Cl_9^{3-}$, we have limited our comparison of calculated and observed features for these complexes to the E′-symmetry mode analogous to that reported for $Cr_2Cl_9^{3-}$. Note here that we infer the "very strong" IR signal seen for crystalline $K_3W_2Cl_9$, $Cs_3W_2Cl_9$, and $(Bu_4N)_3W_2Cl_9$ at 311−313 cm^{-1}, and originally assigned to a mode of A_2'' symmetry,[13] to be of E′ symmetry by analogy with the observed laboratory spectra for $Cr_2Cl_9^{3-}$ and $Mo_2Cl_9^{3-}$, consistent with the results of our DFT calculations which, regardless of technique, invariably yield spectra with the highest-frequency active mode having this symmetry. Other problems relating to the original assignment of $W_2Cl_9^{3-}$ vibrational modes[13] have been noted previously by Black et al.[162] For both $Mo_2Cl_9^{3-}$ and $W_2Cl_9^{3-}$, VWN is closest to the identified laboratory spectral features, while B-LYP and RPBE again perform the most poorly.

The data displayed in Table 5, while not statistically overwhelming, show the same general trends discussed in the subsections above with regard to the reliability of different DFT methods for multiply charged dinuclear complexes, and in this sense, the calculated vibrational frequencies support our contention that an "overbinding" method is better able to compensate for the coulombic distortion suffered by such a complex on its removal from the crystalline environment. We envisage that the orthodox gradient-corrected DFT methods are likely to perform significantly better in determining frequencies for neutral or singly charged dinuclear complexes than they have fared for the multiply charged examples explored here, although we have not tested this assertion in the present work.

2.11. General Appraisal of Method Performance. What can be concluded as a result of the data summarized in Tables 3−5? First, it is apparent that the orthodox gradient-corrected methods which perform very well for neutral and singly charged dinuclear complexes, particularly PW91, PBE, and BP, do not fare well in vacuum-phase calculations on highly charged dinuclear complexes. Only two of eight multiply charged complexes (namely $Mo_2(NCCH_3)_8^{4+}$ and ZORA-corrected $W_2Cl_9^{3-}$, both of which have notably strong metal−metal bonds with multiple bond character), are adequately optimized by any of the orthodox gradient-corrected methods. The optimized geometries for $Cr_2(CH_3)_8^{4-}$, $Mo_2Cl_9^{3-}$, and $Mo_2I_9^{3-}$ are particularly poor.

It is hardly surprising that some of these complexes are difficult to treat using conventional DFT methods. Removed from the crystalline environment, such highly charged species are subjected to severe coulombic stress, and the influence of this stress is to weaken the complex's constituent bonds. When, as is often the case, the metal−metal interaction is intrinsically the weakest bonding interaction present within the complex, M−M bond attenuation and even (as seen for $Cr_2(CH_3)_8^{4-}$) bond rupture within the vacuum-phase geometry are a direct result. The intrusion of these coulombic effects is unwelcome when the intended purpose of DFT calculations is to explore a complex as it exists within a condensed medium such as a solvated or crystalline state. For such purposes, and specifically *w*hen the dinuclear complex of interest bears multiple overall positive or negative charges, our calculations suggest that it is much better to use an "overbinding" method such as VWN or the less extreme VWN+B-LYP rather than an orthodox gradient-corrected method. This strategy is particularly appropriate for investigating properties associated with the metal−metal interaction itself, rather than metal/ligand effects. Metal-centered parameters appropriate in this regard obviously include the optimized M−M bond length on which we have principally focused in the present work, but associated properties such as vibrational modes and magnetic coupling parameters are also pertinent. For vibrational modes, we have found in the present work that both VWN and VWN+B-LYP show generally better applicability than any of the orthodox gradient-corrected functionals, mirroring the trend seen for bond length calculation. This can be rationalized as a result of the somewhat better description (of the energetic

response of the complex to M−M oscillation in the vicinity of the potential energy minimum) by VWN and VWN+B-LYP rather than the orthodox gradient-corrected methods. In previous studies on the multiply charged face-shared dinuclear complexes,[4,5] we have also found that the magnetic properties of these complexes are better treated by local-density methods rather than by gradient-corrected methods: like the metal−metal separation, this is another metal-centered attribute which depends on the interplay between d-orbital localization and delocalization. While the magnetic character of the complexes has not been the direct focus of attention in the present work, it is nevertheless reasonable to suggest that, for highly charged complexes, a method delivering an approximately correct M−M separation is more likely to prove reliable than a method which drastically overestimates the metal−metal distance.

Note that we are not suggesting that the "overbinding" methods VWN and VWN+B-LYP are ideal computational tools for studying multiply charged complexes: no one functional fulfils this description, and as in any computational chemical endeavor the limitations of the technique must be borne in mind. The superior performance of these methods, over orthodox gradient-corrected approaches, for multiply charged species is contingent on the fortuitous cancellation of errors, overbinding versus coulombic stress. This approximate cancellation appears to hold well for triply charged and tolerably well for quadruply charged dinuclear species but may not adhere in calculations on species in higher charge states than these. A more reliable, and more generally applicable, method would involve the explicit inclusion of correction terms for solvent or counterion effects. Our experience to date is that inclusion of such correction factors, combined with the broken-symmetry approach essential for characterizing the competition between metal atom d-electron localization versus delocalization, remains highly impractical for all but the most structurally simple dinuclear complexes.

Concluding Remarks

We have conducted a survey on the performance of several different density functionals, as implemented within the Amsterdam density functional package. Our assessment is based on comparison of the optimized metal−metal separations, obtained from broken-symmetry calculations on a wide variety of dinuclear complexes, with the corresponding bond lengths obtained from previously reported crystallographic structural characterizations. Comparison of calculated and experimentally observed vibrational frequencies has also been undertaken for some of the complexes, and the vibrational results essentially support the conclusions drawn from the more detailed bond length-based analysis.

Our analysis consistently identifies two trends. First, DFT calculations on neutral or singly charged dinuclear complexes are more accurate (in terms of characterizing the metal−metal interaction) when performed using one of the following orthodox gradient-corrected approaches: Perdew−Wang91 (PW91), Perdew−Burke−Ernzerhof (PBE), or Becke−Perdew (BP). Other functionals tested are prone to repeated and significant underestimation (VWN or VWN+B-LYP) or exaggeration (B-LYP, RPBE, or revPBE) of the metal−metal separation. Second, calculations on multiply charged dinuclear complexes are best performed using one of the methods (VWN or VWN+B-LYP) which show significant "overbinding" character, since such functionals provide an approximate correction for gas-phase coulombic distortion from the crystalline geometry of interest for such complexes.

Our survey has also unearthed several examples of complexes whose optimized geometry is highly sensitive to the computational method used. Structures such as $Cr_2(CH_3)_8^{4-}$, $Mo_2Cl_9^{3-}$, $Mo_2I_9^{3-}$, and $Cr_2(O_2CH)_4$ show considerable promise as "problematic" complexes against which the performance of new density functionals, or other computational approaches to transitional metal complex structural characterization, can usefully be assessed.

Acknowledgment. We gratefully acknowledge the Australian Research Council (ARC) for financial support.

IC034525E